International Journal of Communication Networks and Information Security
2024, 16(1), 6442
ISSN: 2073-607X,2076-0930
https://https://ijcnis.org/
Research Article

A Communication Application Design Framework Based on Mesh Network Architecture for Folk Song Dissemination

Xin Liu [1*], Anqi Tang [2]

[1.] DFA Candidate, Doctor of Fine Arts Program in Musicology, International College, Krirk University, Bangkok, Thailand
[2.] Professor, Dr., Doctor of Fine Arts Program in Musicology, International College, Krirk University, Bangkok, Thailand
***Corresponding Author:** liuxinwddmps2022@outlook.com

Citation: X. Liu and A. Tang, "A Communication Application Design Framework Based on Mesh Network Architecture for Folk Song Dissemination," *International Journal of Communication Networks and Information Security (IJCNIS)*, vol. 16, no. 1, pp. 19-32, Apr. 2024.

ARTICLE INFO

Received: 15 November 2023
Accepted: 6 April 2024

ABSTRACT

This document suggests a pair of optimization and enhancement algorithms for Mesh network architecture to foster the spread of folk songs and evaluates these algorithms within a communication design framework. Proposed are communication applications utilizing Mesh network architecture. The average end-to-end delay of the improved expected transmission time metric algorithm is is lower than that of other algorithms; The channel allocation algorithm of wireless mesh network structure improves the throughput by about 16% with the same number of data streams; The real-time reliable data transmission delay of the folk music dissemination framework is significantly lower than that of the non-realtime reliable data network; The mean delay from start to finish in the real-time dependable data transfer within the folk music distribution system is markedly less compared to that in a non-realtime dependable data network.; The folk music communication framework's real-time reliable data transmission experiences an average end-to-end delay, with an average data reception rate surpassing that of non-real-time reliable data, and the real-time reliable data. The rate of receiving usable data from start to finish remains largely unaltered regardless of the amount of communication data; Upon functional testing of the Application (APP), the Central Processing Unit (CPU) usage rate in most tasks remains under 10%; however, during the system's operation, both the occupied memory and CPU usage on the Personal Computer (PC) side is significantly lower. During the operation of the framework, the PC side's occupied memory and CPU usage rate maintain a comparatively steady state.

Keywords: Mesh, Network Architecture, Communication Application Design Framework, Folk Song Dissemination, Real-time Reliable Data

INTRODUCTION

To enhance the spread of folk music, maximizing the use of computer network technology is crucial, and the wireless Mesh network stands out from conventional wireless networks due to its superior transmission efficiency. In recent years, academics, both domestically and internationally, have extensively studied Mesh networks' usage.

Zhang [1] merged his work with two instances of network failures to thoroughly investigate the dependability of nuclear power plants' digital system networks, focusing on aspects like digital network architecture, failure patterns, unusual emergency response plans, mechanisms for blocking network storms, programs for upgrading network switches, and so on. He [2] explores the application of Mesh network technology in fire emergency communication and analyses the network architecture and application advantages of Mesh network technology. Zhao [3] proposed a 3D-Mesh topology interconnection network structure, which supports dynamic reconfigurable configuration with a data path bit width of 32 bit. Yang [4] reviewed the current status of wireless mesh network research in terms of routing and channel allocation. Li Xiao et al., [5] employed the OMNeT++ platform for simulating communication networks to develop a model for simulating wireless sensor networks, utilizing a hybrid Mesh architecture.

This document suggests a Mesh network-based communication application design framework to foster the spread of folk songs. Firstly, three optimization and improvement algorithms for Mesh network structure are proposed in this paper, and two algorithms are tested. Based on the improvement algorithms, a communication application design framework based on a Mesh network structure is proposed, and the design framework is verified through simulation and practical application with a view to contributing to the dissemination of folk songs.

RELATED RESEARCH

Mesh Network Architecture

A wireless mesh network consists of a Mesh Gateway (a node that provides Internet connectivity), a Mesh Router, and a Mesh Client. Networks connected to the Internet through a wireless mesh network can communicate. They use different types of connections between them; out of all the connections, one connection is an in-network connection, i.e. connecting to the Internet through a gateway, and the other connections are wireless or wired connections [7], [8]. The choice of connection is based on the trade-off between cost and performance of the wireless mesh network. The wireless mesh network consists of three basic nodes with different functions, so its structure can be a more flexible and varied hierarchical network based on mesh router nodes, mesh gateway nodes and mesh client nodes with different functions [9].

Improved Algorithm for Mesh Network Structure Optimisation

Load Balancing Oriented Routing Algorithms for Wireless Mesh Network Architecture

Improved Expected Transmission Time Metric Algorithm

Expected Transmission Time (ETT) is developed from the expected transmission count metric (ETX). ETX is a more applicable routing metric for Wireless Sensor Networks (WMNs) proposed by Douglas for the lack of hop count. This metric takes into account the packet loss rate of the link, the difference between symmetric and asymmetric links, and the interference of consecutive hops between multi-hop paths, etc., and can reflect the quality of the transmission link more accurately. The ETX of a link is calculated from the forward and reverse transmission rates using the following formula [10].

$$\mathrm{ETX} = \frac{1}{d_f^* d_r} \tag{1}$$

where is d_f forward delivery rate,

indicating the likelihood of a packet successfully arriving at the subsequent node, and d_r is the reverse delivery rate, which represents the probability that an Acknowledge Character (ACK) packet returned by the next node successfully reaches this node [11]. Each node records the total number of probe packets it receives in the last ω seconds to calculate the link reverse delivery rate in period ω at any time t. The formula is as follows:

$$d_r = \frac{\mathrm{count}\ (t-\omega, t)}{\omega/t} \tag{2}$$

Where $\mathrm{count}\ (t-\omega, t)$ denotes the number of probe packets received by the node in ω seconds, ω/t denotes the total number of probe packets theoretically received by the node in ω seconds.

The ETX metric is as follows:

$$\mathrm{ETX} = \mathrm{ETX} * \frac{S}{B} \tag{3}$$

Where S denotes the number of probe packets received by the node in seconds, and B represents the total link bandwidth.

On the basis of the ETT metric, the Modified Expected Transmission Time Metric (MMETT) formula for node i is proposed as follows:

$$\mathrm{MMETT}\ (i) = \mathrm{ETX}(i)^* \frac{S}{\delta^* BW_i} \begin{cases} \delta = 3, \\ \delta = 1, \end{cases} \tag{4}$$

$$BW_t = \left(1 - \frac{T_{tory}}{T_{buy} + T_{tide}}\right) * TX_{rase} \tag{5}$$

Where the δ factor distinguishes between backbone layer nodes and client layer nodes, T_{buy} represents the remaining bandwidth of the link. T_{tide} represents the node busy duration, T_{tory} represents the node idle duration, and TX_{rase} represents the transmission rate of the link. The above parameters are obtained from the Multiple Access Control (MAC) layer across the layers without sending active probe packets [12].

Node Load Value Metrics

The load level of each node is evaluated by considering the relationship between the average queue length and the maximum queue length of each node. The calculation formula is as follows:

$$L(i) = \frac{\sum_{j=1}^{*} j^{*} QL_{i,j}}{b_i^{*} \sum_{j-1}^{*} j} \tag{6}$$

$$LF(i) = \frac{\sum_{j=1}^{N} L_{ij}}{N} \tag{7}$$

$$LF(i) = \frac{\sum_{j=1}^{N} L_{ij}}{N} \tag{8}$$

Where QL_i is the waiting queue length of the node and is the maximum queue length of the node to be able to process the packets.

Mixed Metric Load Balancing Algorithm (MMLBA) Algorithm Design

As shown in Figure 1, the backbone layer router contains only a gateway that is directly connected to a fixed wired broadband network [13]. We assume that the traffic demand in the network is divided into two categories, one between the client and the Internet and the other from client to client. Each client can form an end-to-end traffic flow from both other routers to the gateway to access the Internet and from multi-hop nodes to the destination. Other imitation parameters are shown in Table 1 below.

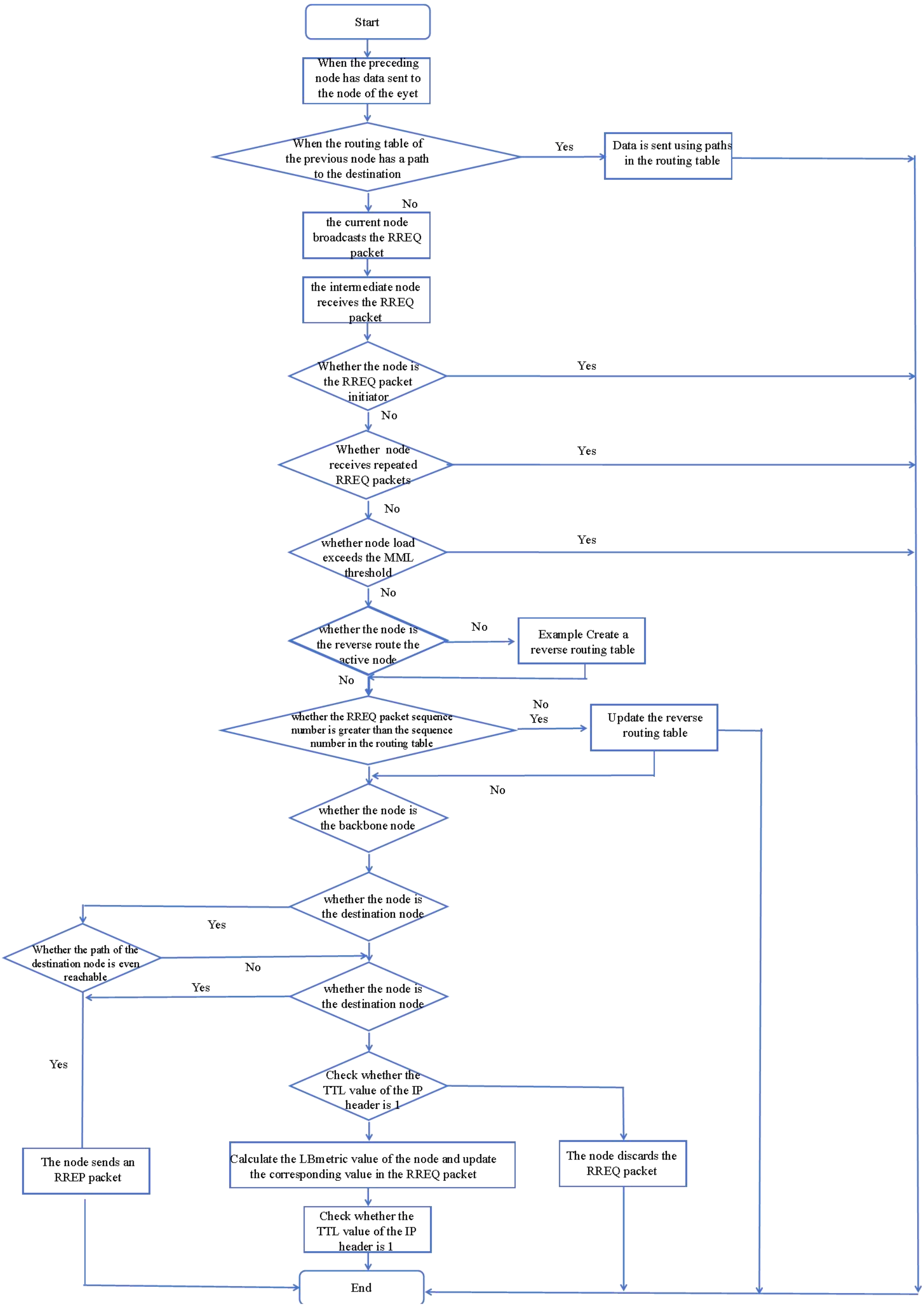
Start
When the preceding node has data sent to the node of the eyet
When the routing table of the previous node has a path to the destination
Yes
Data is sent using paths in the routing table
No
the current node broadcasts the RREQ packet
the intermediate node receives the RREQ packet
Whether the node is the RREQ packet initiator
Yes
No
Whether node receives repeated RREQ packets
Yes
No
whether node load exceeds the MML threshold
Yes
No
whether the node is the reverse route the active node
No
Example Create a reverse routing table
No
whether the RREQ packet sequence number is greater than the sequence number in the routing table
No
Yes
Update the reverse routing table
No
whether the node is the backbone node
whether the node is the destination node
Yes
Whether the path of the destination node is even reachable
No
Yes
whether the node is the destination node
Yes
Check whether the TTL value of the IP header is 1
The node sends an RREP packet
Calculate the LBmetric value of the node and update the corresponding value in the RREQ packet
The node discards the RREQ packet
Check whether the TTL value of the IP header is 1
End

(1) Routing Please Find the Process Diagram

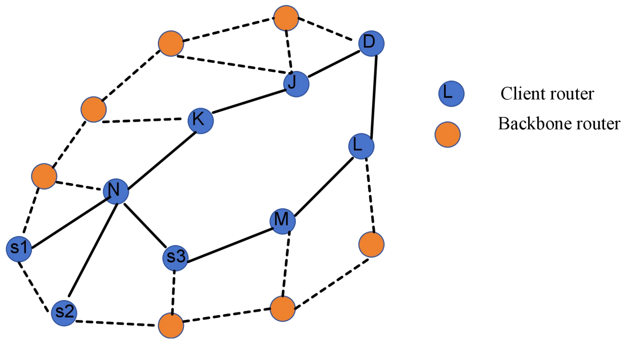

(2) Data Transmission Diagram

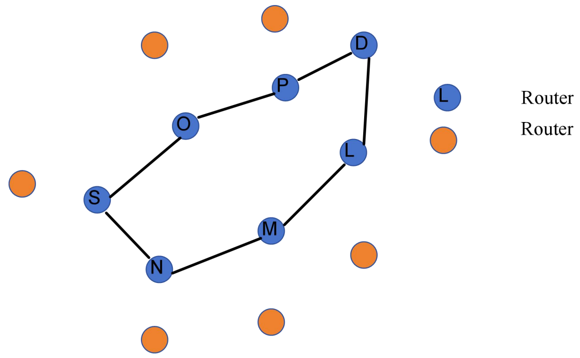

(3) Selection of Road Rules Diagram

Figure 1. MMLBA Algorithm Design

Table 1. Simulation Parameters Table

Simulation Parameters	Parameter Values
Simulation time	200S
Data type	UDP
Packet size	1024bytes
Sending rate	80kbps
Number of backbone layer nodes	20
Number of client nodes	30

Algorithm Testing

This algorithm uses the NS3 network simulation platform for simulation analysis. The network simulation scenario built by NS3 is very similar to the real network. Because NS3 uses C++ class objects to implement the hardware and software facilities of the real network. The simulation platform is the NS3 network simulator. The running platform is Ubuntu 18.04 under the Linux system. The simulation range is 1000*3000m, and the simulation scenario is a hybrid mesh network with fixed bone thousand nodes and randomly moving client nodes. The total number of nodes in the simulation is 50 nodes, and the MAC layer protocol is IEEE802.11b protocol. The service uses Constant Bitrate (CBR) service flow, and the data flow randomly selects the sending and receiving nodes [14], [15], [16].

The average packet loss rate is the ratio of the number of packets lost by all destination nodes to the number of packets sent by all source nodes in the overall network. The formula is as follows:

The average packet loss ratio is the ratio of the number of packets lost by all destination nodes in the overall network to the number of packets sent by all source nodes in the overall network. The formula is as follows:

$$\text{Lossradio}=\frac{\sum_{n=1}^{N} P_n^{ds}-\sum_{n=1}^{N} P_n^{dr}}{\sum_{n=1}^{N} P_n^{ds}} * 100\% \tag{9}$$

Average network throughput represents the proportion between the total packet bits received by all destination nodes in the network and the overall duration of network transmission. The formula is as follows:

$$Throughput = \frac{\sum_{n=1}^{N}\sum_{p=1}^{p_n^*} b_{n,}}{pum}\,(ps) \tag{10}$$

The average end-to-end delay is the ratio of the total delay of packets received by all destination nodes in the overall network to the number of packets received by the destination node. The formula is as follows:

$$Delay = \frac{\sum_{n=1}^{N}\sum_{p-1}^{P_s^t} D_{n,p}}{\sum_{n=1}^{N} P_n^{dr}}\,(\sim ms/packet) \tag{11}$$

The following simulation data are taken as the average of 10 times, by comparing the simulation of the MMLBA algorithm and Long-Reach Inter-Exchange Bundle-High Reliable Protocol (LIB-HRP) algorithm Cooperative Hybrid Routing Protocol (CHRP) algorithm and HMesh algorithm under different numbers of service flows in terms of the average end-to-end delay, average throughput and average network packet loss, the simulation results are shown in Figure 2 below.

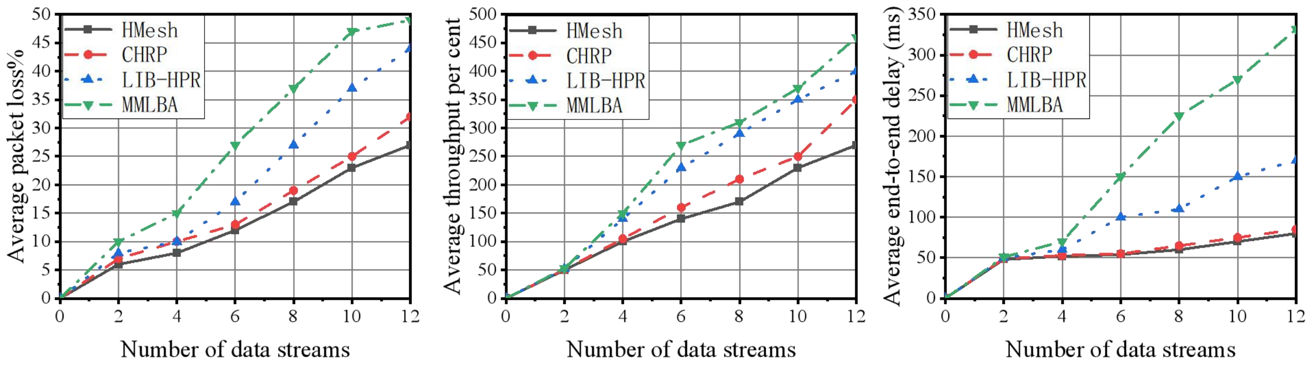

(1) The average packet loss rate varies with the number of data streams sent

(2) Variation of Average Throughput with Number of Data Streams Sent

(3) The average time delay varies with the number of data streams sent.

Figure 2. Simulation Results

Subsequently, a comparison is made of the MMLBA algorithm's simulation, focusing on its average end-to-end delay, throughput, and network packet loss rate, as presented in this paper, alongside other algorithms with data streams set at 4., and different client nodes move at different speeds. The simulation data is taken as the average of 10 results and the simulation results are shown in Figure 3 below.

In hybrid WMN, the overall packet loss rate of the network is increased with the increase in the mobile speed of the client nodes in the network. However, the packet loss rate of the HMesh algorithm is the largest, which is due to the metric of this algorithm being the number of hops; as the network's node's moving speed escalates, the most efficient route for data transfer frequently becomes the client node with fewer hops, resulting in regular disconnections during transmission and b causes a rise in the rate of packet loss; with the increase of the moving speed of the nodes in the network, the average throughput of the network decreases. The average throughput of the network decreases as the speed of nodes increases; the overall average delay of the network increases as the speed of nodes in the network increases. Therefore, the average end-to-end delay of this algorithm is lower than other algorithms.

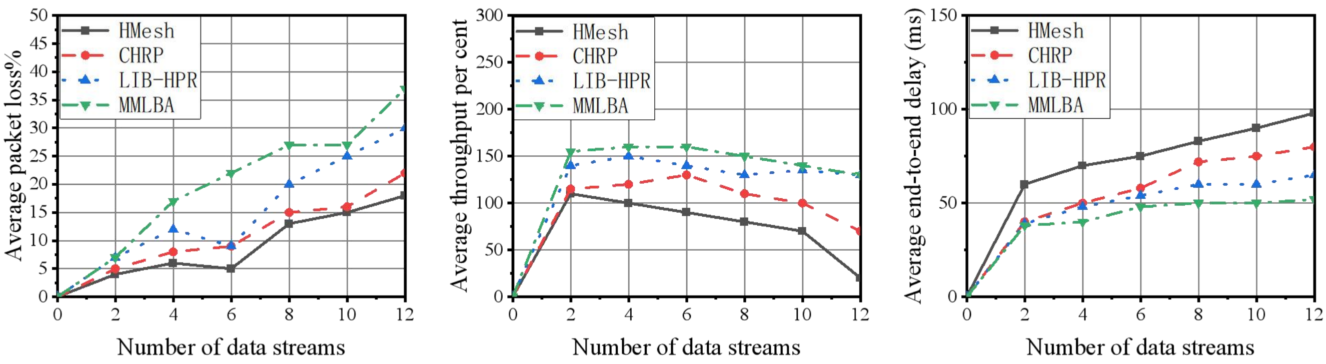

(1) Average packet loss rate varies with client-side node shifts

(2) Average throughput varies with customer-side node shifts

(3)Average time delay varies with client-side node shifts

Figure 3. Simulation Results

Wireless Mesh Network Architecture Channel Allocation Algorithm

System Model

In a WMN network, V is defined as the set of nodes, and E is the set of edges [17]. Cw denotes the set of orthogonal channels for the whole network, the number of elements in the set is w, and each channel is labelled 1,2,3... respectively. w, i.e., Cw={1,2,3... C(v) denotes the set of channels assigned by node v, the number of elements in the set is C(v), and the number of Radio Frequency (RF) interfaces installed in each node is s. Considering the actual situation, i.e., when a node transmits information at a certain moment, the number of channels assigned by the node is impossible to be greater than the number of RF interfaces installed in the node, and at the same time, in order to be able to utilize each RF interface as much as possible and not to cause the wastage of RF interfaces, the number of channels for RF interfaces is fully satisfied [18]. At the same time, in order to be able to use each RF interface as much as possible without causing waste of RF interfaces and to fully satisfy the demand for channel allocation of RF interfaces, it is necessary to make the number of orthogonal channels of the whole network not less than the number of RF interfaces of each node [19], [20]. Then there are:

$$|C(v)| \leq s \leq w \tag{12}$$

$$g(e_{ij}) = \begin{cases} 1 & d_{ij} \leq R_t \\ 0 & d_{ij} > R_t \end{cases} \tag{13}$$

Equation (3.3) denotes $g(e_{ij}) = 1$ when nodes i and j are able to form a link between them and $g(e_{ij}) = 0$ when nodes i and j are not able to form a link between them.

At that time, it does not mean that the two nodes are directly able to communicate; only after allocating a channel for link e_{ij} link it can be used for communication, called a communicable link. The conditions for the formation of a communicable link are shown in equations below:

$$x(e_{ij}) = \begin{cases} k & k \in C_w,\ g(e_{ij}) = 1 \\ 0 & \text{else} \end{cases} \tag{14}$$

$$f(e_{ij}) = \begin{cases} 1 & x(e_{ij}) \neq 0 \\ 0 & x(e_{ij}) = 0 \end{cases} \tag{15}$$

If links e_{ij} and e_{mn} are assigned the same channel, there must be interference between links e_{ij} and e_{mn}. The set of links that may have interference with link e_{ij} is denoted by $I(e_{ij})$. The mathematical definition of $I(e_{ij})$ is shown in equation (16).

$$\forall e_{ij} \in EI(e_g) = \{e_{mn} | e_{mn} \neq e_y \text{且} \min(d_{im}, d_m, d_{jm}, d_{jn}) \leq R_d,\ \ e_{mn} \in E\} \tag{16}$$

Connectivity-based Channel Assignment Model

If the entire network is to be interference-free between links, then the following requirements are to be met when making channel assignments for links:

$$\forall e_{ij} \in E, \forall e_{mn} \in I(e_{ij}) x(e_{mn}) \neq x(e_{ij}) \neq 0,\ \ x(e_{mn}) = x(e_{ij}) = 0 \tag{17}$$

Equation (17) indicates that for any link, there is no link interference in the network if no other link exists within its interference range that is assigned the same channel as the link. The above analysis leads to the optimization model:

$$\{x(e_{ij}) | e_{ij} \in E\} = \arg\max F \quad (18)$$

$$\text{Subject to} L = \sum_{e_q \in E} f(e_{ij})\, e_{ij} \in E \quad (19)$$

$$M = \sum_{e_q \in E} g(e_{ij})\, e_{ij} \in E \quad (20)$$

$$|C(v)| \le s \le w \quad (21)$$

$$g(e_{ij}) = \begin{cases} 1 & d_{ij} \le R_i \\ 0 & d_{ij} > R_t \end{cases} \quad (22)$$

$$x(e_{ij}) = \begin{cases} k & k \in C_w, g(e_{ij}) = 1 \\ 0 & \text{else} \end{cases} \quad (23)$$

$$f(e_{ij}) = \begin{cases} 1 & x(e_{ij}) \ne 0 \\ 0 & x(e_{ij}) = 0 \end{cases} \quad (24)$$

$$x(e_{mn}) \ne x(e_{ij}) \ne 0, x(e_{mn}) = x(e_{ij}) = 0 e_{ij} \in E, e_{mn} \in I(e_{ij}) \quad (25)$$

$$I(e_{ij}) = \{e_{mn} | e_{mn} \ne e_{ij}, \min(d_{i,m}, d_{i,n}, d_{j,m}, d_{j,n}) \le R_d \text{且} e_{mn} \in E\} \quad (26)$$

The above optimization model fully considers the multi-radio and multi-channel characteristics in WMN networks and expresses the system structure, link communication conditions, and interference-free link conditions accurately using mathematical formulas so that an accurate optimization objective can be obtained in the end [21].

Algorithm Design

The specific algorithm flow is shown in Figure 4.

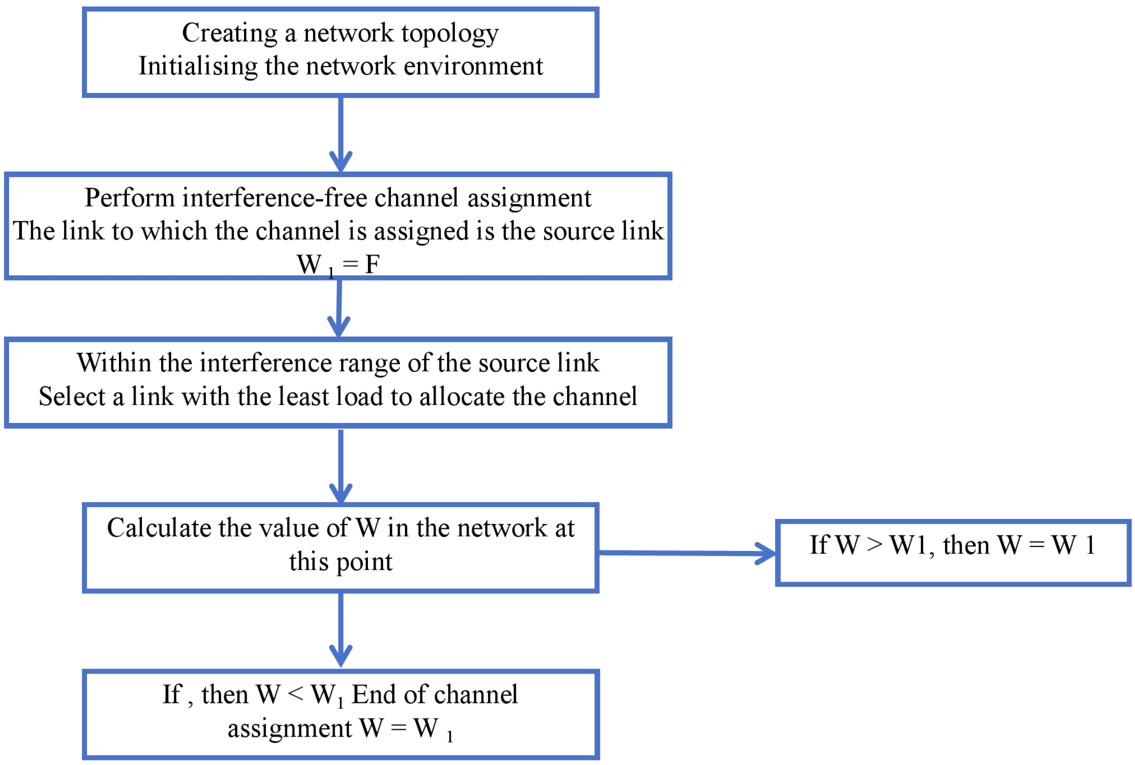

(1) Flowchart of channel assignment algorithm

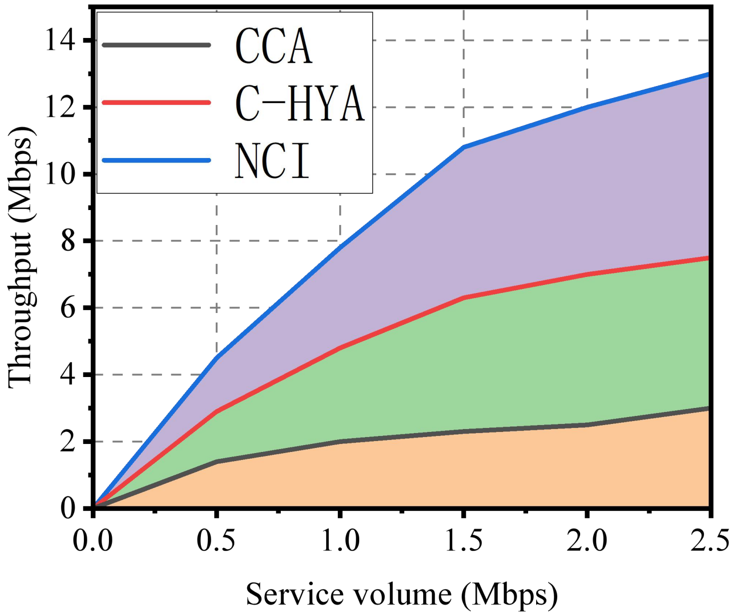

(2) Business volume-throughput relationship for three algorithms

Figure 4. Algorithm Flow and Results

Algorithm Testing

Figure 4(1) shows the changes in the throughput of the networks using the three-channel assignment algorithms as the service volume increases. It can be seen from Figure 4(2) that the throughput of the networks using the three-channel assignment algorithms is able to increase as the service volume of the nodes increases gradually, but the throughput of the network using the NR Cell Identity (NCI) channel assignment algorithm increases more rapidly than that of the networks using the other two channel assignment algorithms. However, the throughput of the network using the NCI channel assignment algorithm increases more rapidly than that of the other two channel assignment algorithms, especially by about 10% compared to the Centralized Hyacinth Channel Assignment (C-HYA) algorithm. This suggests that the network's transmission efficiency is enhanced by the NIC channel assignment algorithm introduced in this study [22].

Figure 5(1) represents the effect of the change in the number of network channels on the network throughput among the three-channel allocation algorithms; from Figure 5(1), it can be seen that as the number of available channels in the network increases, the Clear Channel Assessment (CCA) channel allocation algorithm does not improve the throughput of the network, The reason is that the CCA distributes identical channels across every node in the network, meaning alterations in channel availability do not influence its channel allocation process.

Figure 5(2) shows the effect of the change of network CBR streams on the network throughput in the three-channel allocation algorithms, where the horizontal coordinate indicates the gradual increase of the number of CBR streams in the network from 6 to 16 and the vertical coordinate indicates the change of the throughput.

The diagram illustrates that as the quantity of CBR streams in the network rises, the efficiency of networks employing the trio of channel allocation methods escalates variably, among which the NCI algorithm and the C-HYA algorithm are obviously better than the CCA algorithm, and the NCI channel allocation algorithm mentioned in this paper improves the throughput by about 16% compared to the C-HYA algorithm with the same number of streams.

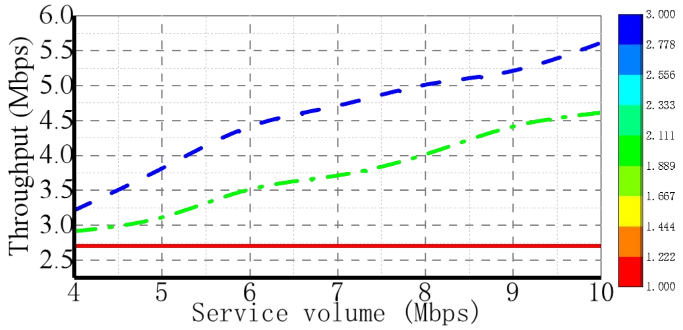

(1) Channel number-throughput relationship for three algorithms

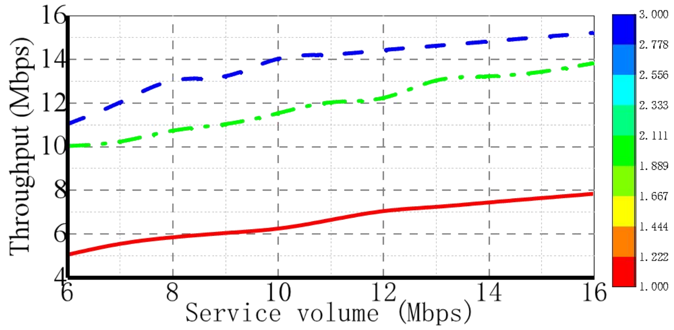

(2) CBR stream-throughput relationship for three algorithms

Figure 5. Simulation Results

METHOD

A Framework for Designing Communication Applications Based on Mesh Network Architecture

Network Structure

According to the significant needs of the folk song dissemination communication framework, this system adopts a hybrid structure of wireless mesh network as the overall topology of the folk song dissemination communication framework. The framework uses the wireless mesh network as the backbone network. The system is mainly composed of two parts: the management body and the folk song lovers. The management body mainly consists of the command centre, routers and the Local Area Network (LAN) for accessing the Internet. The command centre is composed of a series of servers and PC consoles. The command centre is not only able to analyze, process, and display the folk song data transmitted by the folk singers but also to interact with the folk singers by voice and video for instruction [23], [24]. The folk song enthusiasts ' part mainly includes mesh routing node Mesh Portalpoint (MP), mesh access point MAP, mesh gateway, and various wireless terminal devices, such as mobile phones, computers, recorders, etc. Mesh routing node MP is responsible for network routing, relaying and forwarding, and mesh access point MAP is responsible for connecting to various wireless terminal devices in the network. Wireless Mesh Gateway (MG) is responsible for data forwarding between the wireless mesh network and the wired network of folk song enthusiasts. Various wireless terminals mainly include wireless data terminals, wireless voice terminals, and wireless cameras, which are responsible for voice and video collection and processing [25].

Logical Structure

The folk song dissemination communication framework consists of three main components: personnel location and navigation, voice communication and video surveillance.

Personnel Location and Navigation

A personnel location subsystem needs to be designed to obtain the location information of folk music enthusiasts. However, it is slightly different from the voice communication subsystem and video monitoring subsystem, it is not meaningful to use the personnel positioning subsystem alone, it must be used to co-operate with other subsystems [26].

Voice Communication

The voice communication subsystem includes handheld terminals and voice scheduling subsystem software. Through the voice scheduling subsystem, it can control the communication methods with the folk music enthusiasts, such as group call and single call, etc., and it can also notify the folk music enthusiasts of the corresponding real-time information through the form of broadcasting[27], [28].

Video Communications

Modules such as personnel positioning are used to understand the situation and solve the problem through relevant parameters and data such as personnel positioning. Voice modules are used to coordinate with each other through voice communication, and video monitoring is the most intuitive way to understand folk music performance [29]. In the process of folk music dissemination, the video monitoring module uses a wireless mesh network as its bearer network and all the video data are transmitted through the wireless mesh network. The camera accesses the wireless mesh network through the wireless communication module and transmits the data from the front-end camera to the command centre through Transmission Control/User Datagram Protocol (TCP/UDP Protocol). The command centre makes corresponding judgment decisions based on the video of the folk music performance, and at the same time, the command centre can send control command commands to the camera to modify the parameters of the camera, reboot and other tasks [30].

RESULT

Network Simulation Test

The results of the average end-to-end transmission delay of real-time reliable data and non-real-time reliable data obtained from the simulation tests are shown in Figure 6(1). The diagram illustrates that with the rise in the percentage of real-time dependable data within the node's total data from 10% to 90%, the delay in transmitting real-time reliable data from start to finish escalates from roughly 36ms to 49ms, with the delay in transmitting non-real-time reliable data from start to finish escalates from roughly 101ms to 168ms.

Figure 6 illustrates that as the amount of real-time dependable data in the total volume of communication data rises, the mean rate of end-to-end data transmission for real-time reliable data remains consistent. edited to exceed 99.9%, The mean rate of receiving end-to-end data for non-realtime reliable data stands at approximately 96.3%, and this rate is steadier compared to that for non-realtime reliable data. Information.

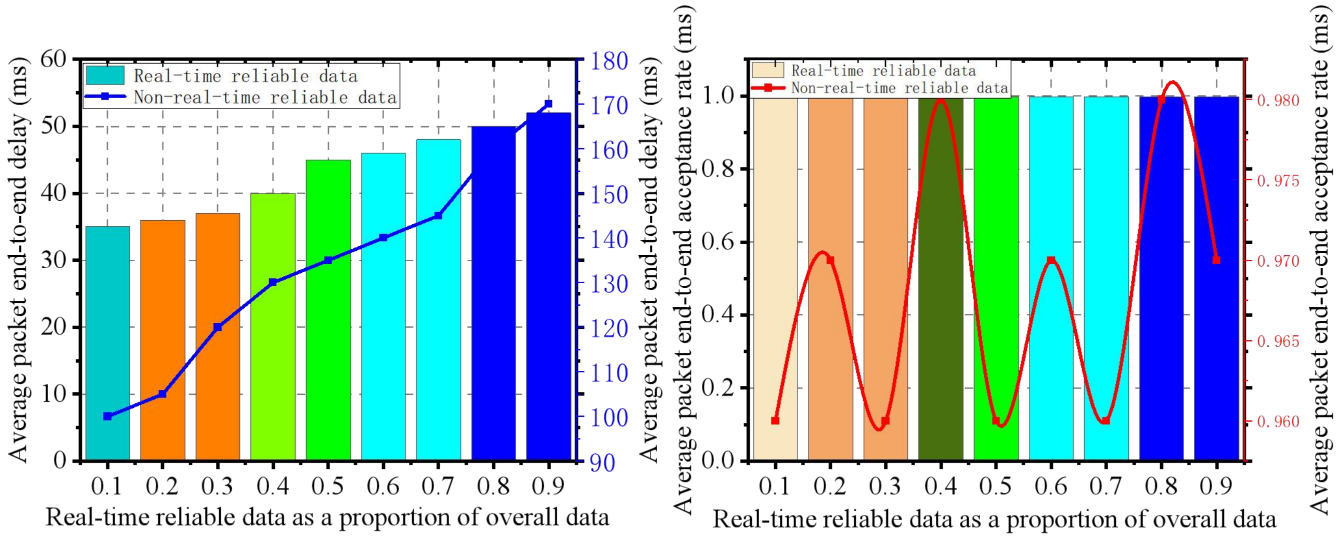

(1) Average packet end-to-end delay (2) Average packet end-to-end acceptance rate

Figure 6. Average End-to-end Communication Delay and Average Packet Reception Rate for All Nodes of the Network

Figure 7 displays the mean transmission delay from start to finish and the average rate of reception for both real-time and non-real-time dependable data from 121 distribution terminal nodes, tested in simulations at 10%, 50%, and 90% of the total data. Refer to Figure 7, Figure 8 and Figure 9.

Figure 7(1) and Figure 7(2) displays the simulated outcomes of the total average delay for each node, considering that real-time dependable data constitutes 10% of the total data. Outcomes from the simulation regarding the total average reception rate for each node in real-time scenarios Dependable data, constituting 10% of the total data, are depicted in Figure 7(3) and Figure 7(4). The end-to-end average reception rates of real-time reliable data and non-real-time reliable data of 121 nodes tested in the simulation are 99.79% and 96.13%, respectively, of which the average reception rate of real-time reliable data transmission of node 29 is the minimum 99.92%, the average reception rate of real-time reliable data transmission of node 32 is the maximum of 99.99%, Node 86's average rate of receiving non-real-time reliable data stands at a low of 90.1%, while node 123 achieves a peak average reception rate of 99.3% for non-real-time reliable data.

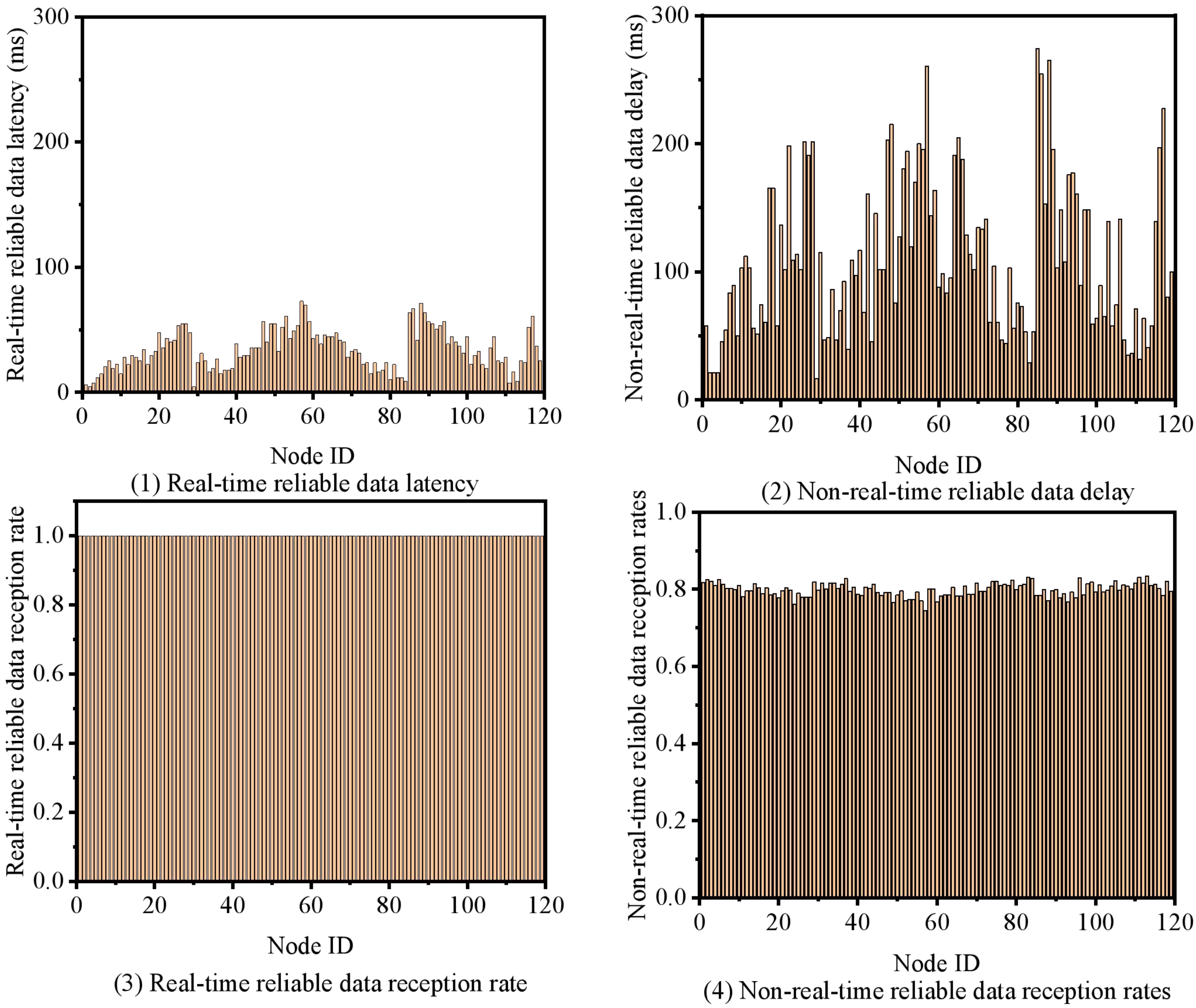

Figure 7. A Percentage of 10 Percent

The simulation results of the end-to-end average delay of each node when real-time reliable data accounts for 50% of the overall data are shown in Figure 8(1) and Figure 8(2). In the simulation, 121 nodes experienced an average transmission delay of 43.1ms for real-time reliable data and 139.9ms for non-real-time reliable data across the entire system, respectively, of which the average delay of real-time reliable data transmission of node 5 is the smallest 12.6ms, and the maximum average delay of non-real-time reliable data of node 86 is 283.4 ms. The simulation results of the end-to-end average reception rate of each node when real-time reliable data accounts for 50% of the overall data are shown in Figure 8(3) and Figure 8(4). In the simulation, 121 nodes exhibited end-to-end average reception rates for both real-time and non-real-time reliable data, which stood at 99.98% and 96.09%, respectively, of which the average reception rate of real-time reliable data transmission of node 119 is 99.90% at minimum, the average reception rate of real-time reliable data transmission of node 85 is 99.99% at maximum, the average reception rate of non-real-time reliable data of node 86 is 90.1%.

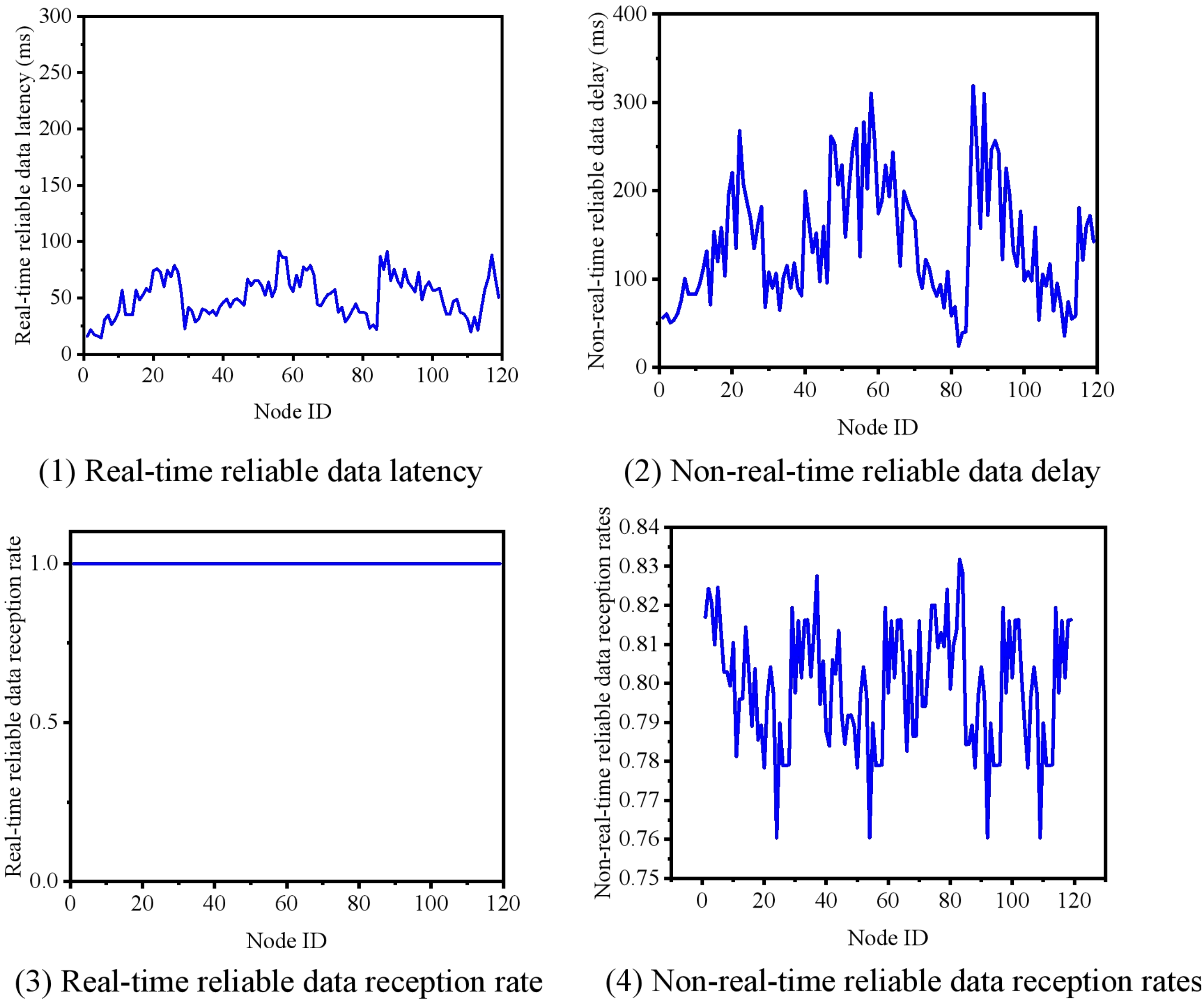

Figure 8. 50 Percent Share

The simulation results of the end-to-end average delay of each node when real-time reliable data accounts for 90% of the overall data are shown in Figure 9(1). In the simulation, 121 nodes experienced an average transmission delay of 52.7ms for real-time reliable data and 175.1 ms for non-real-time reliable data from start to finish, respectively, among which the average delay of real-time reliable data transmission of node 4 is the minimum of 14.9 ms, and the maximum average delay of non-real-time reliable data of node 87 is 367.1 ms.

Results from simulations depicting the total average reception rate for each node, considering that real-time dependable data comprises 90% of the total data, are presented in 10.

In the simulation, the total average rate of receiving both real-time and non-real-time reliable data from 121 nodes was 99.96% and 96.21%, respectively, respectively, of which the average reception rate of real-time reliable data transmission of node 60 is 99.91% minimum, the average reception rate of real-time reliable data transmission of node 123 is 99.98% maximum, the average reception rate of non-real-time reliable data of node 54 is 90.1%, and node 2 has a maximum average reception rate of 99.3% for non-real-time reliable data.

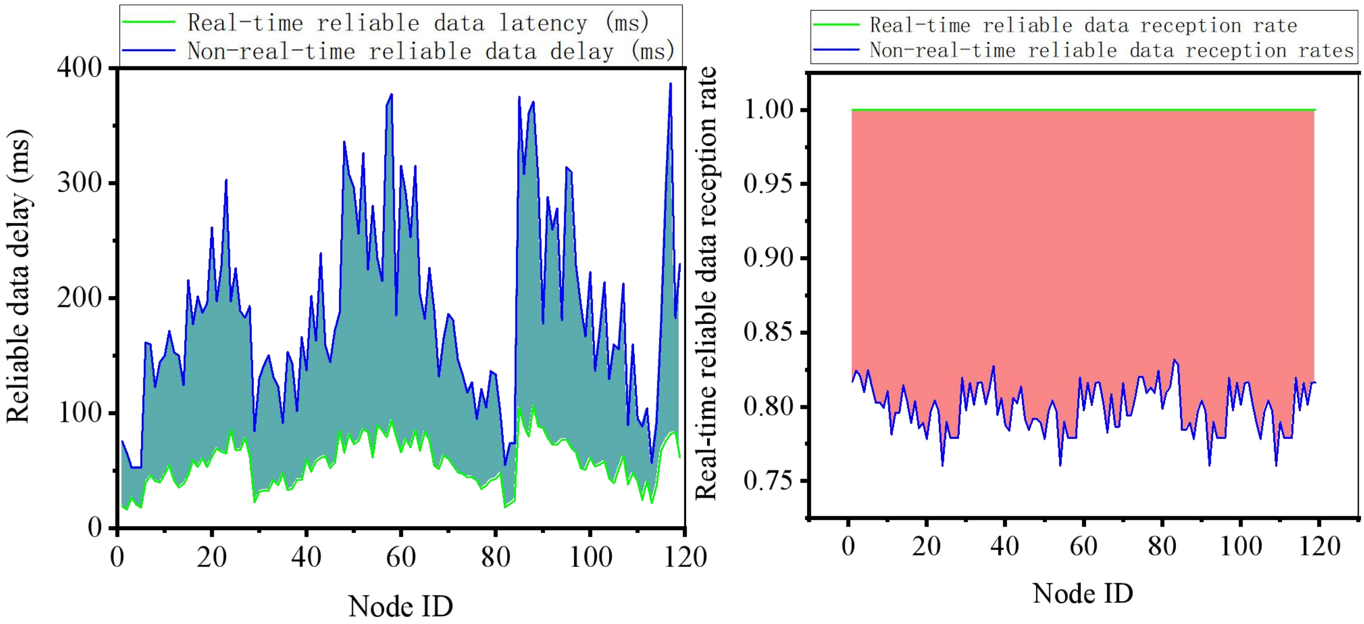

(1) Data latency (2) Data reception rates

Figure 9. 90 Percent

Actual Performance Tests

Android Client Testing

In the performance test for the Android terminal of folk music enthusiasts, this paper tests the occupied memory and CPU occupancy during the operation of the APP using the design framework. Install the Android client application on the Huawei Honor model CAM-AL00 test machine and perform various operations in the Android APP such as registration, login, adding friends, group creation, chatting and sending files, etc. Capture the APP's occupied memory size and CPU occupancy rate through the Emmagee tool. The test results are shown in Figure 10.

As can be seen from Figure 10(1), during the functional test, the captured data shows that the APP consumes about 100MB of memory, and there is no memory leakage during the test. As shown in Figure 10(2), the captured data shows that the CPU occupancy rate of the APP is below 10% in most of the operations during the functional tests, but there are some operations that may result in a relatively high CPU occupancy rate, but it is still below 15%.

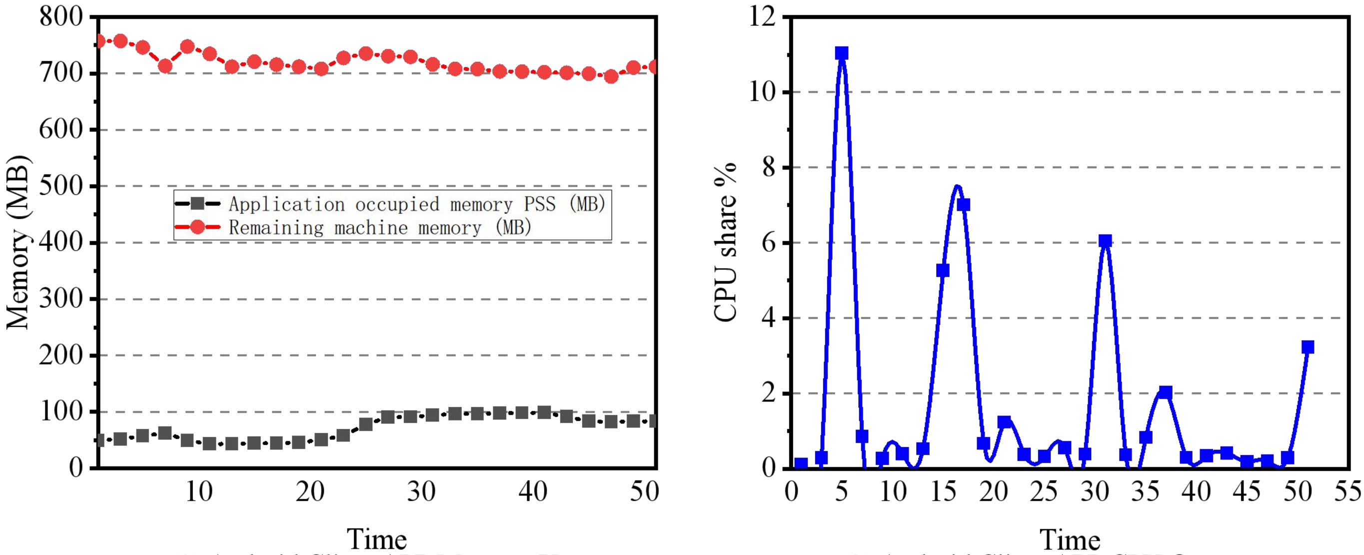

(1) Android Client APP Memory Usage (2) Android Client APP CPU Occupancy

Figure 10. Memory Usage of the Client Design Framework

PC Test

By simulating the user after a series of operations, screenshots of the PC application's memory and CPU usage are taken. The test results are shown in Figure 11, which shows that the memory and CPU usage of the PC application is at a relatively stable level when the framework is running.

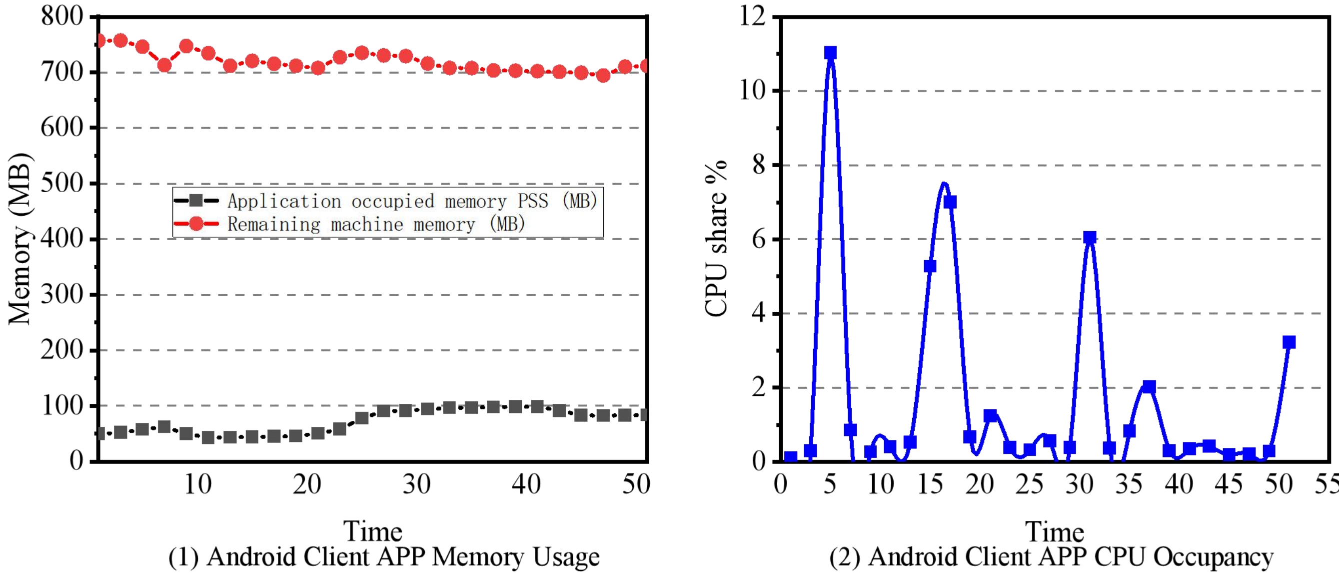

Figure 11. PC Client Design Framework Occupancy Rate

CONCLUSION

In this paper, based on the mesh network structure, a design framework for communication applications based on the mesh network structure is proposed. The design framework is verified through simulation as well as practical applications, and the specific conclusions are as follows:

Compared to other methods, the enhanced algorithm for measuring expected transmission time exhibits a reduced average delay from start to finish.

The wireless mesh network structure channel allocation algorithm has a better performance by increasing the throughput by about 16% with the same number of data streams.

The folk song propagation communication framework is mainly composed of three parts: personnel positioning and navigation, voice communication and video monitoring

In the folk music dissemination framework, the delay in transmitting data reliably in real-time is markedly less than that in the non-real-time reliable data network, and the average delay from end to end in real-time reliable data is less influenced by the amount of data considered, whereas the average delay in non-real-time dependable data transmission from start to finish is more influenced by the amount of data accounted for.

The average data reception rate of real-time reliable data transmission in the folk music propagation framework is higher than that of non-real-time reliable data. The real-time reliable data end-to-end reception rate of all nodes is higher than 99.9%.

During the functional test of the APP, it can be seen from the captured data that the CPU occupancy rate of most operations is below 10%, but some operations may cause a relatively high CPU occupancy rate, but it is still below 15%; when the framework is running, the occupied memory and CPU occupancy rate of the PC side are at a relatively stable level.

ETHICAL DECLARATION

Conflict of interest: No declaration required. **Financing:** No reporting required. **Peer review:** Double anonymous peer review.

REFERENCES

[1] L. L. Zhang, P. Li, and F. Yang, "Research on reliability improvement of digital network in nuclear power plants," (in Chinese), *Equipment Management and Maintenance*, no. 19m, pp. 82-86, 2023.

[2] C. H. He, "Application of mesh network technology in fire emergency communication," (in Chinese), *Firefighting Community (electronic version)*, vol. 8, no. 17, pp. 56-58, 2022.

[3] Z. G. Zhao, W. Li, Z. B. Dai, and J. G. Geng, "Research on coarse-grained logic array based on 3D-Mesh interconnection network," (in Chinese), *Electronic Technology Application*, vol. 42, no. 5, pp. 27-31, 2016.

[4] L. Yang, R. F. Liu, "A review of routing and channel assignment for wireless mesh networks," (in Chinese), *Journal of Guiyang College (Natural Science Edition)*, vol. 8, no. 4, pp. 33-39+43, 2013.

[5] X. Li, Z. H. Ling, Y. Zuo, "Exploration of path determinism in MESH structured wireless sensor networks," (in Chinese), *Automation Instrumentation*, vol. 34, no. 1, pp. 10-13, 2013.

[6] S .Y. Shahdad, A. Sabahath, and R. Parveez, "Architecture, issues and challenges of wireless mesh network," in *2016 International Conference on Communication and Signal Processing (ICCSP)*, Apr. 2016, pp. 557-560.

[7] M. F. Rabbi, M. T. Rahman, M. A. Uddin, and G. A. Salehin, "An efficient wireless mesh network: A new architecture," in *2006 International Conference on Communication Technology*, Nov. 2006, pp. 1-5.

[8] J. Bicket, D. Aguayo, S. Biswas, and R. Morris, "Architecture and evaluation of an unplanned 802.11 b mesh network," in *Proceedings of the 11th annual International Conference on Mobile Computing and Networking*, Aug. 2005, pp. 31-42.

[9] C. K. Zachos, J. Loo, and S. Khan, "Wireless mesh network: Architecture and protocols," *Mobile Ad Hoc Networks: Current Status and Future Trends*, vol. 2, pp. 425-448, 2016.

[10] M. Eslami, O. Karimi, and T. Khodadadi, "A survey on wireless mesh networks: Architecture, specifications and challenges," in *2014 IEEE 5th Control and System Graduate Research Colloquium*, Aug. 2014, pp. 219-222.

[11] F. Martignon, S. Paris, and A. Capone, "DSA-mesh: A distributed security architecture for wireless mesh networks," *Security and Communication Networks*, vol. 4, no. 3, pp. 242-256, 2011.

[12] S. Sakamoto, R., Obukata, T. Oda, L. Barolli, M. Ikeda, and A. Barolli, "Performance analysis of two wireless mesh network architectures by WMN-SA and WMN-TS simulation systems," *Journal of High Speed Networks*, vol. 23, no. 4, pp. 311-322, 2017.

[13] M. Bano, A. Qayyum, R. N. B. Rais, and S. S. A. Gilani, "Soft-mesh: A robust routing architecture for hybrid SDN and wireless mesh networks," *IEEE Access*, vol. 9, pp. 87715-87730, 2021.

[14] J. R. Parvin, "An overview of wireless mesh networks," *Wireless Mesh Networks-Security, Architectures and Protocols*, 2019, doi: 10.5772/intechopen.83414.

[15] S. K. Gupta, A. R. Wani, S. Kumar, A. Srivastava, and D. Sharma, "Wireless mesh network security, architecture, and protocols," in *Security and Privacy Issues in Sensor Networks and IoT*, Hershey, PA, USA: IGI Global, 2020, ch. 1, pp. 1-27.

[16] C. S. Choi, F. Baccelli, and G. de Veciana, "Densification leveraging mobility: An IoT architecture based on mesh networking and vehicles," in *Proceedings of the Eighteenth ACM International Symposium on Mobile Ad Hoc Networking and Computing*, Jun. 2018, pp. 71-80.

[17] F. Ahmed et al., "Wireless mesh network IEEE802.11s," *International Journal of Computer Science and Information Security (IJCSIS)*, vol. 14, no. 12, pp. 803-809. 2016.

[18] E. Longman, O. Cetinkaya, M. El-Hajjar, and G. V. Merrett, "Mesh networking for intermittently powered devices: Architecture and challenges," *IEEE Network*, vol. 36, no. 3, pp. 122-128, 2022.

[19] S. Bahirat and S. Pasricha, "METEOR: Hybrid photonic ring-mesh network-on-chip for multicore architectures," *ACM Transactions on Embedded Computing Systems (TECS)*, vol. 13, no. 3s, pp. 1-33, 2014.

[20] J. Zhang, "Proposal of free space optical mesh network architecture for broadband access," in *2002 IEEE International Conference on Communications. Conference Proceedings. ICC 2002 (Cat. No. 02CH37333)*, vol. 4, Apr. 2002, pp. 2142-2145.

[21] N. Gokulraj and K. Umapathy, "5G wireless mesh network 802.11 s load balancing architecture for 802.11 Bgn radio-PCI interface," *Procedia Computer Science*, vol. 87, pp. 252-257, 2016.

[22] K. Kosek-Szott, J. Gozdecki, K. Loziak, M. Natkaniec, S. Szott, and M. Wagrowski, "ViMeNO: A Virtual wireless mesh network architecture for operators," in *2013 International Conference on Wireless Information Networks and Systems (WINSYS)*, Jul. 2013, pp. 1-8.

[23] Q. Wan and J. Liu, "Smart-home architecture based on Bluetooth mesh technology," *IOP Conference Series: Materials Science And Engineering*, vol. 322, no. 7, p. 072004, 2018.

[24] B. Kim et al., "Tactical network design and simulator with wireless mesh network-based backbone architecture," in *2010 IEEE Long Island Systems, Applications and Technology Conference*, May 2010, pp. 1-

5.

[25]B. Wehbi, A. Laouiti, and A. Cavalli, "A reactive wireless mesh network architecture," in *IFIP Annual Mediterranean Ad Hoc Networking Workshop*, Jun. 2008, pp. 203-214.

[26]F. Licandro and G. Schembra, "Wireless mesh networks to support video surveillance: Architecture, protocol, and implementation issues," *EURASIP Journal on Wireless Communications and Networking*, vol. 2007, pp. 1-13, 2007.

[27]A. Cilfone, L. Davoli, L. Belli, and G. Ferrari, "Wireless mesh networking: An IoT-oriented perspective survey on relevant technologies," *Future Internet*, vol. 11, no. 4, p. 99, 2019.

[28]M. T. Zhou et al., "TRITON: High-speed maritime wireless mesh network," *IEEE Wireless Communications*, vol. 20, no. 5, pp. 134-142, 2013.

[29]R. Ramanathan, C. Servaes, W. Ramanathan, A. Dusia, and A. S. Sethi, "Long-range short-burst mobile mesh networking: Architecture and evaluation," in *2019 16th Annual IEEE International Conference on Sensing, Communication, and Networking (SECON)*, Jun. 2019, pp. 1-2.

[30]J. Núñez-Martínez and J. Mangues-Bafalluy, "A survey on routing protocols that really exploit wireless mesh network features," *Journal of Communications*, vol. 5, no. 3, pp. 211-231, 2010.